Appendix B: Faith Valley Greenhouse Gas Monitoring Report

2021, 2022, and 2023 Carbon Flux at Faith Valley Meadow

Evan Wolf

2024 January 29

Carbon dioxide flux was measured at 12 plots distributed across a ~10 ha area of Faith Valley. The plots represent the herbaceous vegetation within the riparian corridor in Faith Valley and are all located within 100 m of the West Fork of the Carson River. Significant stands of willow also occur within Faith Valley, and these are not included in this analysis. Flux rates were measured in late June and early July near the peak of the growing season in 2021, 2022, and 2023. A cylindrical chamber 30 cm in diameter and 30 cm tall, connected to an infrared gas analyzer (IRGA) was used to measure CO_2 flux rates. The clear chamber was placed on the plots in full mid-day sunlight for 1-2 minutes to obtain a net ecosystem exchange (NEE) measurement. After a chamber-off rest period, the chamber was completely obscured to block all sunlight, and placed back on each plot to measure the ecosystem restoration (ER) rate. The photosynthetic rate, gross primary productivity (GPP), was calculated by subtracting ER from NEE.

Flux rates were calculated by fitting a quadratic equation to the CO_2 concentration measured once per second within the chamber. The flux rates from the plots were averaged to give a measurement of mid-summer peak CO2 flux for the entire 10 ha meadow area. The plot-measured flux rates were used to calibrate annual hourly-time-step models for ER and GPP. The snow-free growing season when plant growth and GPP occurs at Faith Valley, was determined from local weather records and remote imagery to run from May 1 to Dec 5 (219 days) in 2021, from May 1 to Oct 28 (181 days) in 2022, and from June 15 to Dec 5 (174 days) in 2023.

Three environmental variables were used to model CO_2 flux: Soil temperature, solar irradiance, and enhanced vegetation index (EVI). Soil temperature was measured at Stanislaus Meadow 12 miles away and 200 feet higher in elevation in a similar meadow setting. Based on prior studies, approximately 1/3 of total peak-season ER is composed of microbial respiration of soil organic matter, whose rate is determined primarily by soil temperature (Wickland et al. 2001, Gao et al. 2017). The remaining 2/3 of growing-season ER come from plant respiration and microbial decomposition of plant root exudates, both of which are directly related to plant growth and fluctuate daily and seasonally with the rhythms of plant productivity and phenology (Han et al. 2014).

These plant-related ER components were modelled as a function of plant biomass and productivity. Herbaceous above-ground biomass rises from zero just after snowmelt to a peak in mid-summer and falls back to zero through the growing season and is modelled using EVI. Productivity fluctuates diurnally, as the sun rises and sets, and is modelled by solar irradiance modified by seasonal biomass represented by EVI. Solar irradiance was measured hourly at the Highlands Meadow meteorological station 15 miles from Faith Valley and 1200 feet higher in elevation, in a similar Sierra meadow landscape. EVI was remotely sensed by the Sentinel-2 satellites and provides a daily measure of meadow greenness. Solar irradiance and EVI were used to model GPP.

The chamber-measured rates of mid-summer GPP and ER were used to calibrate the models based on EVI, solar irradiance, and soil temperature. The lower end of the EVI data was normalized by subtracting the same value from all annual EVI readings such that the new minimum growing season EVI equaled zero. This zero EVI reading represents no greenness, no actively photosynthesizing vegetation, and

results in zero GPP. The new maximum EVI (after the subtraction described above) was multiplied to equal 1 on the day of mid-summer meadow flux chamber readings was 1. All other EVI data in the same year were multiplied by this factor to re-scale the entire year to zero for when no plants were present, to 1 to match field-measured productivity. Field chamber readings were taken as close to peak biomass, and therefore peak EVI, as possible so that the normalized EVI values would peak close to 1. This reduces the number of scaled EVI values >1, which would model GPP > field-measured values. Keeping most scaled EVI between zero and 1 minimizes extrapolation of flux data beyond field-measured or zero-constrained values. This ensures that most modeled GPP values are interpolations between the known value of zero GPP when there are no green plants (EVI = 0), and the field-measured GPP where EVI is set to 1. When solar irradiance is zero, GPP is zero, so no normalization was necessary. The GPP response to irradiance was modeled using a rectangular hyperbola function. GPP was modeled as normalized EVI * GPP ~ irradiance via the rectangular hyperbola function. Field flux readings were taken during mid-day on sunny days near mid-summer to ensure that the GPP readings are close to maximum values, again to minimize extrapolation in the GPP ~ irradiance model.

Soil temperature measured hourly was used to model the soil-only component of ER. Because ER does not go to zero at 0 degrees Celsius, we used an average of under-snow readings from similar wetland settings to estimate the respiration rate at 0°C of 0.11 g CO_2 m^{-2} hr^{-1} (Wickland et al. 2001, 2006, Knowles et al. 2016, Blackburn et al. 2021). ER response to soil temperature was modeled as an exponential Q_{10} (the factor by which a 10°C increase in temperature will increase the rate of decomposition) function (Wickland et al. 2001).

GPP and ER were modeled on an hourly time step during the years 2021, 2022, and 2023. To describe the modeled rates through the year, the growing season was divided into four equal periods of 44 to 55 days each, depending on year, that correspond to significant phenological plant development: emergence, peak growth, flowering, and senescence. The model output was summarized in each of these four growing-season periods and winter to ensure that its output was conforming to expected trends in seasonal plant development. The measured environmental variables of soil temperature, solar irradiance and normalized EVI are shown in relation to the phenological periods (Figure 1). Values of NEE greater than zero indicate a net transport of CO_2 from the meadow into the atmosphere, whereas negative values of NEE represent net transport of CO_2 into the meadow plant/soil ecosystem.

The main difference between years was in length of growing season, with 2021 having about 40 more snow-free days than either 2022 or 2023. The long growing season in 2021 resulted in a net storage of 19.5 Mg CO2 in the 10 ha herbaceous meadow area. Shorter snow-free growing seasons led to net losses of 61.8 and 49.0 Mg CO2 in 2022 and 2023, respectively. Over the three years of this study, a net total of 91.3 Mg CO2 are estimated to have been lost from the 10 ha of herbaceous meadow in Faith Valley, an annual average loss rate of 30.4 Mg CO2 per year. There were no detectable effects of the restoration efforts on the GHG flux in Faith Valley. The interannual variance was so large that any smaller site-specific changes were not seen. In addition, the beaver dam analog treatments were installed in 2022 and the following winter of 2022-23 was one of the largest on record. The subsequent snow-melt peak flow damaged omany of the dams, with repairs and additional BDA installation occurring in fall 2023.

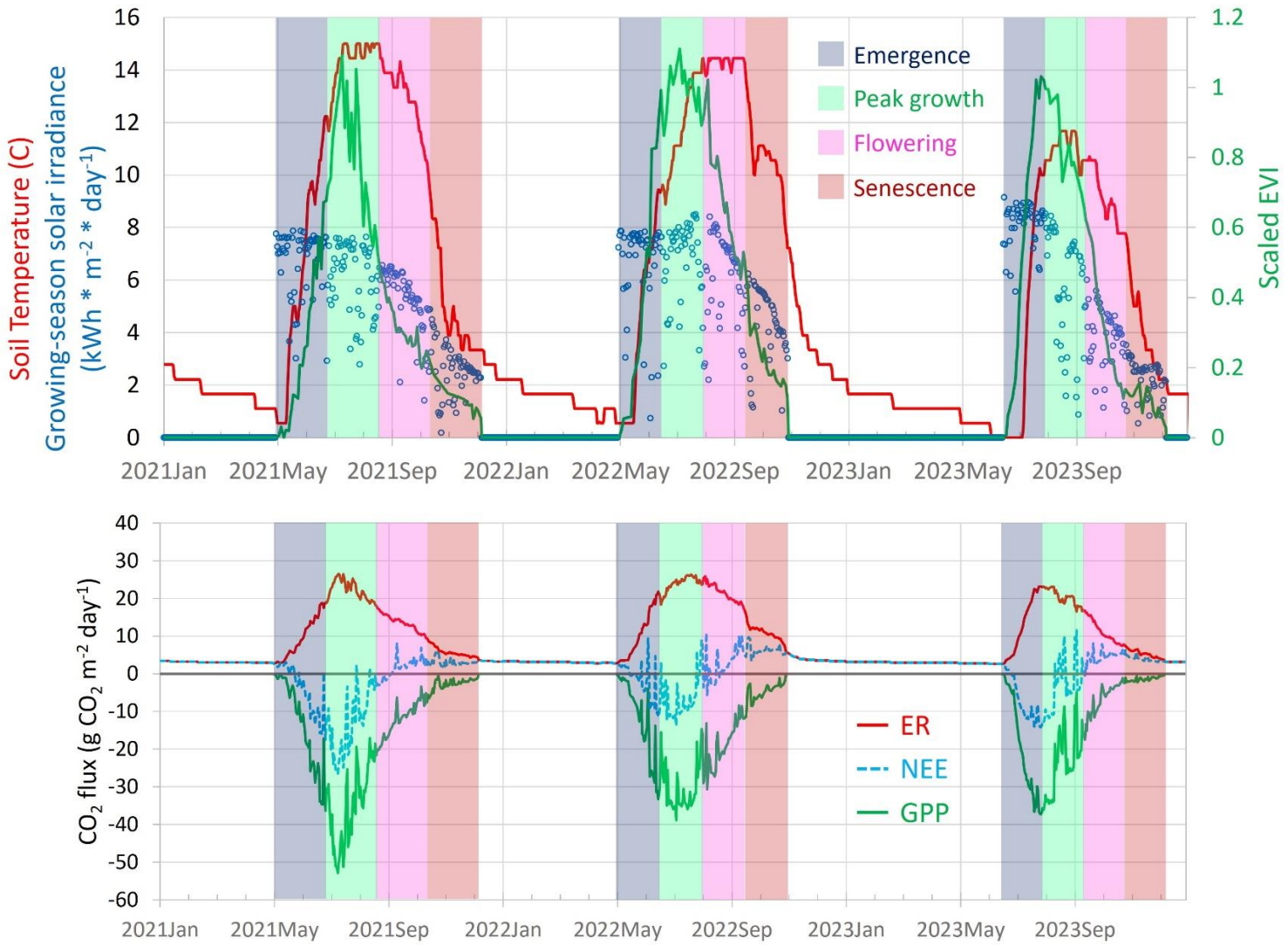

Figure 1. Three-year time series of environmental variables (upper panel) and modeled CO_2 flux (lower panel). Soil temperature was used to model ecosystem respiration (ER) and daily solar irradiance and normalized EVI were used to model gross primary productivity (GPP). The sum of ER and GPP is net ecosystem exchange (NEE). In the lower panel, negative values represent CO_2 moving into the meadow ecosystem and positive values are CO_2 leaving the meadow into the air. ER is always positive and GPP is always negative. Most of the winter irradiance values are not shown, to avoid clutter, because no GPP occurs during the winter.

Table 1. Annualized CO_2 budget per square meter and scaled to the 10 ha (24.71 acre) herbaceous meadow section for 2021, 2022, and 2023, and the growing-season and winter periods in each.

		Days	ER CO_2 flux (kg CO_2 / m^2)	GPP CO_2 flux (kg CO_2 / m^2)	NEE CO_2 flux (kg CO_2 / m^2)	Mg CO_2-eq lost (+) or stored (-) in 10 ha meadow	Emissions MTCO2e/acre/year	Change in soil carbon (24.71 acres) MTCO2e/year
2021	emergence	54.8	0.489	-0.673	-0.184	-18.4		
	peak growth	54.8	1.218	-1.937	-0.719	-71.9		
	flowering	54.8	0.747	-0.668	0.080	8.0		
	senescence	54.8	0.309	-0.142	0.167	16.7		
	winter	146.0	0.461	0.000	0.461	46.1		
	2021 annual total	365.0	3.225	-3.420	-0.195	-19.5	-0.790	-19.5
2022	emergence	45.3	0.452	-0.515	-0.063	-6.3		
	peak growth	45.3	1.074	-1.396	-0.322	-32.2		
	flowering	45.3	0.975	-0.859	0.116	11.6		
	senescence	45.3	0.504	-0.229	0.276	27.6		
	winter	184.0	0.612	0.000	0.612	61.2		
	2022 annual total	365.0	3.617	-2.999	0.618	61.8	2.502	61.8
2023	emergence	43.5	0.543	-0.825	-0.283	-28.3		
	peak growth	43.5	0.881	-1.032	-0.151	-15.1		
	flowering	43.5	0.502	-0.310	0.193	19.3		
	senescence	43.5	0.230	-0.059	0.171	17.1		
	winter	191.0	0.560	0.000	0.560	56.0		
	2023 annual total	365.0	2.716	-2.226	0.490	49.0	1.981	49.0
	3-year total:		9.557	-8.645	0.913	91.3	3.694	91.3
	3-year annual average:		3.186	-2.882	0.304	30.4	1.231	30.4

References

Blackburn, D. A., A. J. Oliphant, and J. D. Davis. 2021. Carbon and Water Exchanges in a Mountain Meadow Ecosystem, Sierra Nevada, California. Wetlands 41:1–17.

Gao, X., X. Mei, F. Gu, W. Hao, H. Li, and D. Gong. 2017. Ecosystem respiration and its components in a rainfed spring maize cropland in the Loess Plateau, China. Scientific Reports 7.

Han, G., Y. Luo, D. Li, J. Xia, Q. Xing, and J. Yu. 2014. Ecosystem photosynthesis regulates soil respiration on a diurnal scale with a short-term time lag in a coastal wetland. Soil Biology and Biochemistry 68:85–94.

Knowles, J. F., P. D. Blanken, and M. W. Williams. 2016. Wet meadow ecosystems contribute the majority of overwinter soil respiration from snow-scoured alpine tundra. Journal of Geophysical Research G: Biogeosciences 121:1118–1130.

Wickland, K. P., R. G. Striegl, M. A. Mast, and D. W. Clow. 2001. Carbon gas exchange at a southern Rocky Mountain wetland, 1996–1998. Global Biogeochemical Cycles 15:321–335.

Wickland, K. P., R. G. Striegl, J. C. Neff, and T. Sachs. 2006. Effects of permafrost melting on CO2 and CH4 exchange of a poorly drained black spruce lowland. Journal of Geophysical Research: Biogeosciences 111.